the support of the Acción Integrada Hispano-Francesa, W. Butler for the X-ray data collection, and A. H. Francis for recording solid-state visible spectra.

Registry No. $(Bu_4N)[Rh_2(cod)_2Dcbp]$, 136823-79-5; $(Me_4N)[Ir_2(cod)_2Dcbp]$, 118859-85-1; $(Pr_4N)[Ir_2(cod)_2Dcbp]$, 136823-80-8; $(Bu_4N)[Ir_2(cod)_2Dcbp]$, 118611-33-9; $(Me_4N)[Rh_2(CO)_4Dcbp]$, 136823-81-9; $(Bu_4N)[Rh_2(CO)_4Dcbp]$, 136823-82-0; $(TTF)[Rh_2(CO)_4Dcbp]$, 136823-83-1; $(Me_4N)[Ir_2(CO)_4Dcbp]$, 118611-42-0; $(Pr_4N)[Ir_2(CO)_4Dcbp]$, 136823-84-2; $(Bu_4N)[Ir_2(CO)_4Dcbp]$, 118611-40-8; $(Me_4N)[Rh_2(CO)_2(PPh_3)_2Dcbp]$, 136823-86-4; $(Bu_4N)[Rh_2(CO)_2(PPh_3)_2Dcbp]$, 136890-85-2; $[Rh_2(CO)_4Dcbp]$, 118611-35-1; $(Pr_4N)[Ir_2(CO)_4Dcbp]_2$, 136823-88-6; $(Bu_4N)[Ir_2(CO)_4Dcbp]_2$, 136890-86-3; $[Rh(\mu\text{-Cl})(cod)]_2$, 12092-47-6; $[Ir(\mu\text{-Cl})(cod)]_2$, 12112-67-3; $[Rh(\mu\text{-OMe})(cod)]_2$, 12148-72-0; $[Ir(\mu\text{-OMe})(cod)]_2$, 12148-71-9.

Supplementary Material Available: Tables S1-S4, listing thermal parameters for all non-hydrogen atoms, calculated hydrogen positions, and complete distances and angles (4 pages); Table S5, listing calculated and observed structure factors (11 pages). Ordering information is given on any current masthead page.

Contribution from Anorganische Chemie I, Ruhr-Universität, D-4630 Bochum, Germany, Institut für Physikalische Chemie, Technische Hochschule, D-6100 Darmstadt, Germany, and Allgemeine Anorganische und Analytische Chemie, Universität-Gesamthochschule Paderborn, D-4790 Paderborn, Germany

Synthesis, Electrochemistry, and Magnetic and Spectroscopic Properties of an Exchange-Coupled $Fe^{III}Ni^{II}Fe^{III}$ Complex. Crystal Structure of $[L_2Fe_2(dmg)_3Ni](PF_6)_2\cdot 0.5CH_3OH$ (L = 1,4,7-Trimethyl-1,4,7-triazacyclononane; dmg = Dimethylglyoximate(2-))

Phalguni Chaudhuri,*,† Manuela Winter,† Beatriz P. C. Della Vêdova,† Peter Fleischhauer,‡ Wolfgang Haase,‡ Ulrich Flörke,§ and Hans-Jürgen Haupt§

Received January 3, 1991

The trimetallic complex $[L_2Fe^{III}_2Ni^{II}(dmg)_3](PF_6)_2\cdot 0.5CH_3OH$, where L is the cyclic amine 1,4,7-trimethyl-1,4,7-triazacyclononane and dmg is the dianion of dimethylglyoxime, has been synthesized and its structure determined by X-ray diffraction methods as having a tris(dimethylglyoximato)nickelate(II) bridging ligand. The complex crystallizes in monoclinic space group $C2/c$ with cell constants a = 29.711 (7) Å, b = 12.569 (4) Å, c = 14.951 (3) Å, β = 119.93 (1)°, V = 4838 Å^3, and Z = 4. The high-spin iron(III) centers have six-coordinate N_3O_3 and the nickel center has six-coordinate N_6 environments, with an Fe···Ni separation of 3.491 (3) Å and an Fe···Fe separation of 6.982 (2) Å. The closest *inter*molecular Fe···Fe separation is 7.37 Å. The X-ray structure confirms that a linear trinuclear complex with an Fe–Ni–Fe angle of 179.4 (2)° has been formed. The compound has also been studied with infrared and electronic spectroscopy, cyclic voltammetry, and variable-temperature (4–284 K) magnetic susceptibility measurements. Analysis of the susceptibility data yields an antiferromagnetic interaction (J_{Fe-Ni}) between adjacent Fe(III) and Ni(II) centers and a weak antiferromagnetic interaction (J_{Fe-Fe}) between the terminal iron(III) centers. The following parameter values are obtained: $J_{Fe-Ni} = -32$ (2) cm^{-1}, $J_{Fe-Fe} = -5$ (1) cm^{-1} for the perchlorate salt; $J_{Fe-Ni} = -29$ (2) cm^{-1}, $J_{Fe-Fe} = -5$ (1) cm^{-1} for the hexafluorophosphate salt. The electronic ground state has been established to have $S = 4$. The effect of J_{Fe-Fe}, which raises the energy of the $S = 4$ level and lowers the energy of the $S = 3$ level on the energy-splitting pattern, has been discussed. The cyclic voltammograms of the $Fe^{III}Ni^{II}Fe^{III}$ complex reveal two quasi-reversible one-electron oxidation and two reversible one-electron reduction processes which have been assigned to the following equilibria:

$$Fe^{III}Ni^{II}Fe^{III} \underset{+e}{\overset{-e}{\rightleftharpoons}} Fe^{III}Ni^{III}Fe^{III} \underset{+e}{\overset{-e}{\rightleftharpoons}} Fe^{III}Ni^{IV}Fe^{III} \qquad Fe^{III}Ni^{II}Fe^{III} \underset{-e}{\overset{+e}{\rightleftharpoons}} Fe^{II}Ni^{II}Fe^{III} \underset{-e}{\overset{+e}{\rightleftharpoons}} Fe^{II}Ni^{II}Fe^{II}$$

Introduction

Exchange-coupled clusters of transition-metal ions are relevant to many different scientific areas,[1-15] ranging from chemistry to solid-state physics and to biology. There is a clear interest from the bioinorganic community, because an increasing number of active centers in metalloproteins are found to contain more than one metal atom. Antiferromagnetic exchange coupling has been observed in different biomolcules,[7-15] e.g. dicopper sites[7-9] in hemocyanin, tyrosinase, and laccase and diferric sites in methemerythrin[10] and ribonucleotide reductase,[11] and heterobimetallic sites of Fe(III) and Cu(II) in cytochrome oxidase.[13-15] In another area of research, there is an intensive effort to design and understand new "molecular magnets", which is mainly directed toward the development of materials with novel properties.[3,6]

Magnetic and EPR data on heteropolymetallic complexes are much less numerous than those dealing with homopolymetallic compounds, particularly Cu(II) compounds, primarily due to a lack of fully structurally characterized compounds.[5,6] New exchange pathways can be expected for heteropolynuclear complexes, where unusual sets of magnetic orbitals can be brought in close proximity; hence investigations of a series of heteropolynuclear complexes might be more informative in comparison to those of

† Universität Bochum.
‡ Technische Hochschule Darmstadt.
§ Universität-Gesamthochschule Paderborn.

(1) *Magneto-Structural Correlations in Exchange Coupled Systems*; Willett, R. D., Gatteschi, D., Kahn, O., Eds.; NATO ASI Series C, Vol. 140; Reidel: Dordrecht, The Netherlands, 1985.
(2) Hatfield, W. E. In *Theory and Applications of Molecular Paramagnetism*; Boudreaux, E. A., Mulay, L. N., Eds.; Wiley: New York, 1976; p 350.
(3) Kahn, O. *Angew. Chem.* **1985**, *97*, 837.
(4) Sinn, E. *Coord. Chem. Rev.* **1970**, *5*, 313.
(5) Bencini, A.; Gatteschi, D. *EPR of Exchange Coupled Systems*; Springer Verlag: Berlin, 1990.
(6) Kahn, O. *Struct. Bonding* **1987**, *68*, 89.
(7) Solomon, E. I. In *Metal Clusters in Proteins*; Que, L., Jr., Ed.; American Chemical Society: Washington, DC, 1988; p 116.
(8) *Biological and Inorganic Copper Chemistry*; Karlin, K. D., Zubieta, J., Eds., Adenine Press: Guilderland, NY, 1983 and 1986.
(9) Petersson, L.; Angstrom, J.; Ehrenberg, A. *Biochim. Biophys. Acta* **1978**, *526*, 311.
(10) Dawson, J. W.; Gray, H. B.; Hoenig, H. E.; Rossman, G. R.; Schreder, J. M.; Wang, R. H. *Biochemistry* **1972**, *11*, 461.
(11) Petersson, L.; Graslund, A.; Ehrenberg, A.; Sjoberg, B. M.; Reichard, P. *J. Biol. Chem.* **1980**, *255*, 6705.
(12) Solomon, E. I.; Penfield, K. W.; Wilcox, D. E. *Struct. Bonding* **1983**, *53*, 1.
(13) Cohen, I. A. *Struct. Bonding* **1980**, *40*, 1.
(14) Malström, B. G. In *Metal Ion Activation of Dioxygen*; Spiro, T. G.; Ed.; Wiley: New York, 1980; Chapter 5.

0020-1669/91/1330-4777$02.50/0

homopolynuclear complexes. The field of heteropolynuclear complexes with different paramagnetic centers is still limited today by the small number of known and fully structurally characterized compounds and by relative difficulty of synthesizing new compounds. Hence the design of heteropolymetallic complexes has for a long time been a challenging field for coordination chemists. In general, such a synthesis[16] requires either the use of metal complexes as ligands[17] for a simple metal salt or the use a stepwise reaction of two different metal ions with polynucleating ligands[18] having dissymmetric coordination sites.

In order to understand the factors that determine the spin physics of the different metal-containing biomolecules and with the aim of providing some answers to questions regarding the effectiveness of polyatomic bridging ligands like oximes and their metal complexes in propagating exchange interactions, we have synthesized a series of dimethylglyoximato-bridged linear heterotrinuclear complexes of general formula $[L_2Fe^{III}{}_2M^{II}(dmg)_3]^{2+}$ (M = Zn, Cu, Ni, Co, Fe, Mn). This has been accomplished by stepwise reactions of the LFe unit with the in situ prepared $M^{II}(dmg)_3{}^{4-}$ ion, where L represents the simple tridentate cyclic amine 1,4,7-trimethyl-1,4,7-triazacyclononane, which coordinates facially in octahedral complexes.

The paucity of tris(oximato)metalate(II) anions as bridging ligands in coordination chemistry is surprising.[19] Recently we have described a series of trinuclear complexes containing $[M^{II}(dimethylglyoximato)_2]^{2-}$ (M = Cu, Ni, Pd) as bridging ligands.[20] The subject of this paper is the antiferromagnetic exchange-coupled integer spin system of $[L_2Fe^{III}{}_2(dmg)_3Ni^{II}]X_2$ (X = ClO_4, PF_6). We report here the synthesis and magnetic, spectroscopic, and electrochemical properties of the aforementioned compound, together with its X-ray structure. Throughout this paper, the trinuclear complexes are denoted by the respective metal centers only; the terminal and the bridging ligands are omitted for simplicity.

Experimental Section

Materials and Methods. The macrocycle 1,4,7-trimethyl-1,4,7-triazacyclononane was prepared as previously described.[21] All other starting materials were commercially available and were of reagent grade. Elemental microanalyses (C, H, N) were performed by the Microanalytical Laboratory, Ruhr-Universität, Bochum. Iron was determined spectrophotometrically by using pyridine-2,6-dicarboxylic acid; nickel was determined gravimetrically as Ni(dimethylglyoximate)$_2$. The perchlorate anion was determined gravimetrically as tetraphenylarsonium(V) perchlorate. Electronic absorption spectra were measured on a Perkin-Elmer Lambda 9 spectrophotometer in solution. Fourier transform infrared spectroscopy on KBr pellets was performed on a Perkin-Elmer 1720X FT-IR instrument.

Magnetic susceptibilities of powdered samples were recorded on a Faraday-type magnetic balance using a sensitive Cahn RG electrobalance in the temperature range 4.2–284.5 K. The applied magnetic field was ≈0.58 T. Details of the apparatus have already been described elsewhere.[22] Experimental susceptibility data were corrected for the underlying diamagnetism. Corrections for diamagnetism were estimated as -514×10^{-6} and -589×10^{-6} cm^3/mol for the perchlorate **1** and the hexafluorophosphate **2** salts, respectively.

Table I. Crystallographic Data for $[(C_9H_{21}N_3)_2Fe_2Ni(C_4N_2H_6O_2)_2](PF_6)_2\cdot 0.5CH_3OH$

formula	$[C_{30}H_{60}N_{12}O_6P_2F_{12}Fe_2Ni]\cdot 0.5CH_3OH$
fw	1161.24
space group	$C2/c$
a, Å	29.711 (7)
b, Å	12.569 (4)
c, Å	14.951 (3)
β, deg	119.93 (1)
V, Å^3	4838.7
Z	4
D_{calcd}, g cm^{-3}	1.594
$F(000)$	2400
R	0.095
R_w	0.075
T, °C	23
λ(Mo K, graphite monochromated), Å	0.710 73
μ, mm^{-1}	1.14

Cyclic voltammetry experiments were performed with a Princeton Applied Research Model 173 potentiostat–galvanostat driven by a Model 175 universal programmer. Voltammograms were recorded on a Kipp & Zonen XY recorder, Model BD 90. Fast voltammograms (≥1 V s^{-1}) were recorded on a Gould OS 4200 digital storage oscilloscope. The supporting electrolyte was 0.1 M $NBu^n{}_4PF_6$ in methylene chloride or acetonitrile. A standard three-electrode cell was employed with a glassy-carbon working electrode, a platinum-wire auxiliary electrode, and a Ag/AgCl (saturated LiCl in ethanol) reference electrode. Measurements were made under an argon atmosphere at ambient temperature. At the beginning of each experiment a cyclic voltammogram of the solution containing only the supporting electrolyte was measured. Solid samples of the trinuclear complexes were added to this solution and dissolved under stirring to achieve a concentration of ≈10^{-3} M of the electroactive component. The potential of the reference electrode was determined to be −0.06 V vs NHE by using the ferrocenium(1+)/ferrocene couple as the internal standard.

Preparation of Compounds. Method 1. $[(C_9H_{21}N_3)_2Fe_2Ni(C_4N_2H_6O_2)_3](ClO_4)_2$ (1). All operations were carried out under anaerobic conditions. Ferrous acetate (0.17 g, 1.0 mmol) was added to a degassed solution of 1,4,7-trimethyl-1,4,7-triazacyclononane (0.17 g, 1.0 mmol) in 40 mL of methanol under vigorous stirring. The resulting suspension was stirred at room temperature for 2 h to give a pale yellow solution. The resulting solution was charged with solid samples of 0.12 g (0.5 mmol) of $Ni(CH_3COO)_2\cdot 4H_2O$, 0.17 g (1.5 mmol) of dimethylglyoxime, and 1 mL of triethylamine. The suspension was refluxed for 0.5 h and then filtered in the air to remove precipitated Ni(dmgH)$_2$. Sodium perchlorate hydrate (0.4 g) was added, and the dark brown solution was kept at 4 °C. After 24 h, dark brown crystals were collected by filtration and air-dried. Yield: 400 mg (38%).

Anal. Calcd for $C_{30}H_{60}N_{12}O_{14}Cl_2Fe_2Ni$: C, 34.18; H, 5.74; N, 15.95; ClO_4, 18.87; Fe, 10.60; Ni, 5.56. Found: C, 34.1; H, 5.7; N, 15.7; ClO_4, 19.0; Fe, 10.8; Ni, 5.4.

$[(C_9H_{21}N_3)_2Fe_2Ni(C_4N_2H_6O_2)_3](PF_6)_2\cdot 0.5CH_3OH$ (2). Complex **2** was obtained similarly to complex **1** with sodium hexafluorophosphate (400 mg) instead of sodium perchlorate used as the anion source. Dark brown crystals we obtained. Yield: 530 mg (≈46%).

Anal. Calcd for $[C_{30}H_{60}N_{12}O_6P_2F_{12}Fe_2Ni]\cdot 0.5CH_3OH$: C, 31.55; H, 5.38; N, 14.47; Fe, 9.62; Ni, 5.06. Found: C, 31.5; H, 5.4; N, 14.3; Fe, 9.8; Ni, 5.2.

Method 2. A suspension of $(C_9H_{21}N_3)FeCl_3$[28] (0.28 g, 0.84 mmol), $NiCl_2\cdot 6H_2O$ (0.19 g, 0.79 mmol), and dimethylglyoxime (0.28 g, 2.4 mmol) in methanol (40 mL) was refluxed for 2 h. The red-brown Ni(dmgH)$_2$ was filtered off. After addition of either $NaClO_4\cdot H_2O$ (0.4 g) or $NaPF_6$ (0.37 g) to the clear dark brown solution, the solution was kept in a closed vessel for 24 h at 4 °C to obtain dark brown crystals of **1** or **2**. Yield: 300 mg (29%) for **1**; 240 mg (21%) for **2**.

Caution! Although we experienced no difficulties with the perchlorate salt, the unpredictable behavior of perchlorate salts necessitates extreme caution in their handling.

Crystal Structure Determinations. A brown black crystal of $[(C_9H_{21}N_3)_2Fe_2Ni(C_4N_2H_6O_2)_3](PF_6)_2\cdot 0.5CH_3OH$ with dimensions of 0.04 × 0.11 × 0.34 mm was mounted on a Nicolet R3m/V diffractometer. Preliminary examinations showed that the crystal belonged to the monoclinic crystal system, space group $C2/c$. The lattice parameters were obtained at 23 °C by a least-squares refinement of the angular settings ($10° \le 2\theta \le 26°$) of 27 reflections. The data are summarized in Table I. The data were corrected for Lorentz and polarization effects,

(15) *Biophysical Chemistry of Dioxygen Reactions in Respiration and Photosynthesis*; Vänngard, T., Ed.; Cambridge University Press: Cambridge, England, 1988; see also references therein.
(16) Casellato, U.; Vigato, P. A.; Fenton, D. E.; Vidali, M. *Chem. Soc. Rev.* **1979**, *8*, 199.
(17) (a) Gruber, S. J.; Harris, C. M.; Sinn, E. *J. Inorg. Nucl. Chem.* **1968**, *30*, 1805. (b) Selbin, J.; Ganguly, L. *Inorg. Nucl. Chem. Lett.* **1969**, *5*, 815.
(18) (a) Pilkington, N. H.; Robson, R. *Aust. J. Chem.* **1979**, *23*, 2225. (b) Okawa, H.; Tanaka, M.; Kida, S. *Chem. Lett.* **1974**, 987. (c) Lintvedt, R. L.; Glick, M. D.; Tomlonovic, B. K.; Gavel, D. P. *Inorg. Chem.* **1976**, *15*, 1646.
(19) (a) Chakravorty, A. *Coord. Chem. Rev.* **1974**, *13*, 1. (b) Singh, C. B.; Sahoo, B. *J. Inorg. Nucl. Chem.* **1974**, *36*, 1259. (c) Okawa, H.; Koikawa, M.; Kida, S.; Luneau, D.; Oshio, H. *J. Chem. Soc., Dalton Trans.* **1990**, 469.
(20) Chaudhuri, P.; Winter, M.; Della Vêdova, B. P. C.; Bill, E.; Trautwein, A.; Gehring, S.; Fleischhauer, P.; Nuber, B.; Weiss, J. *Inorg. Chem.* **1991**, *30*, 2148.
(21) Wieghardt, K.; Chaudhuri, P.; Nuber, B.; Weiss, J. *Inorg. Chem.* **1982**, *21*, 3086.
(22) Merz, L.; Haase, W. *J. Chem. Soc., Dalton Trans.* **1980**, 875.

Table II. Atomic Coordinates (×10⁴) and Equivalent Isotropic Displacement Parameters (Å² × 10³) for $[C_{30}H_{60}N_{12}O_6Fe_2Ni](PF_6)_2 \cdot 0.5CH_3OH$

	x	y	z	U(eq)[a]
Ni(1)	0	3403 (3)	2500	27 (1)
Fe(1)	1049 (1)	3418 (2)	2061 (2)	32 (1)
O(1)	345 (3)	3240 (8)	899 (7)	34 (3)
O(2)	925 (4)	4655 (8)	2696 (8)	42 (3)
O(3)	1010 (4)	2333 (8)	2931 (7)	37 (3)
N(1)	−33 (4)	2990 (9)	1142 (8)	26 (3)
N(2)	455 (5)	4667 (10)	2659 (9)	32 (3)
N(3)	644 (4)	2474 (1)	3239 (8)	30 (3)
N(4)	1244 (5)	4489 (10)	1113 (10)	41 (4)
N(5)	1910 (5)	3656 (12)	3134 (10)	50 (4)
N(6)	1378 (5)	2231 (11)	1431 (10)	44 (4)
C(1)	−374 (5)	2285 (11)	571 (10)	26 (4)
C(2)	−381 (6)	1705 (14)	−324 (10)	49 (5)
C(3)	267 (5)	5596 (12)	2551 (11)	35 (4)
C(4)	513 (6)	6611 (13)	2507 (11)	54 (5)
C(5)	762 (5)	2069 (11)	4123 (11)	29 (4)
C(6)	1239 (6)	1417 (14)	4764 (12)	60 (5)
C(7)	1692 (7)	5127 (15)	1904 (14)	62 (6)
C(8)	2103 (7)	4506 (15)	2749 (13)	59 (6)
C(9)	2108 (7)	2593 (15)	3144 (14)	67 (6)
C(10)	1931 (7)	2121 (15)	2102 (13)	63 (6)
C(11)	1245 (8)	2730 (16)	410 (14)	76 (6)
C(12)	1401 (7)	3856 (14)	497 (13)	57 (5)
C(13)	805 (6)	5191 (14)	447 (12)	59 (5)
C(14)	2006 (7)	3945 (14)	4186 (12)	67 (6)
C(15)	1115 (6)	1217 (13)	1259 (13)	61 (6)
P(1)	1851 (2)	1239 (5)	8531 (5)	64 (3)
F(1)	1264 (6)	961 (15)	7942 (13)	176 (12)
F(2)	2011 (7)	110 (12)	8504 (13)	185 (13)
F(3)	1803 (6)	1506 (21)	7510 (9)	215 (13)
F(4)	1904 (6)	973 (13)	9595 (12)	149 (12)
F(5)	2414 (4)	1603 (15)	9068 (10)	146 (9)
F96)	1677 (6)	2355 (12)	8687 (13)	147 (12)
C(20)	0	162 (51)	7500	225 (26)
O(20)	291 (18)	689 (36)	8236 (34)	193 (19)[b]

[a] Equivalent isotropic U defined as one-third of the trace of the orthogonalized U_{ij} tensor. [b] Occupation factor 0.5.

but it was not necessary to account for crystal decay. An empirical absorption correction[23] was carried out (ψ-scans). The scattering factors[24] for neutral non-hydrogen atoms were corrected for both the real and the imaginary components of anomalous dispersion. The structure was solved by conventional Patterson and Fourier-difference syntheses. The structure was refined by a least-squares technique; the function minimized was $\sum w(|F_o| - |F_c|)^2$ where $w = 1/\sigma^2(F) + 0.0001F^2$. Idealized positions of H atoms bound to carbon atoms were calculated (C–H = 0.96 Å) and included in the refinement cycle with a common isotropic thermal parameter (U_{iso} = 0.080 Å²). Fe, Ni, P, and F atoms were refined anisotropically. The enclosed methanol solvate molecule lies with its carbon atom on a 2-fold axis, the oxygen atom being statistically disordered over two sites and refined with site occupancy factor 0.5. A maximum of 0.8 e/Å³ in the final ΔF map lies near an Fe position. Final positional parameters are presented in Table II, while selected interatomic distances and angles are given in Table III.

Results and Discussion

Preparation and Characterization of Complexes. The pale yellow solution[25] obtained from ferrous acetate and the cyclic amine in methanol under argon reacting with the $Ni(dmg)_3^{4-}$ ion, prepared in situ, affords upon addition of the perchlorate or hexafluorophosphate ion in the presence of air dark brown crystals of $[L_2Fe_2(dmg)_3Ni]X_2$ (X = ClO_4 (**1**), PF_6 (**2**)) in reasonable yield. The function of added triethylamine is to provide a basic medium needed for the deprotonation of the O···H···O groups present in solid $Ni(dmgH)_2$. The presumably square-planar dianionic $Ni(dmg)_2^{2-}$ produced in this way can now coordinate to a further dmg^{2-} anion to produce the bridging ligand $Ni(dmg)_3^{4-}$. The assembled $Ni(dmg)_3^{4-}$ ion can now react with the hydroxo-bridged diiron(II) complex to form the $Fe^{II}Ni^{II}Fe^{II}$ species,[27] which becomes oxidized to the heterotrinuclear $Fe^{III}Ni^{II}Fe^{III}$ species in the presence of oxygen from the air. A similar type of reactivity of the diferrous compound $[L_2Fe_2(OH)(OAC)_2]^+$ has also been observed earlier.[28] Interestingly, the reaction of $LFeCl_3$[28] with the $Ni(dmg)_3^{4-}$ ion, assembled in situ, also affords the desired $Fe^{III}Ni^{II}Fe^{III}$ complex, but in comparatively low yield. The low yield is the result of presumably low concentration of the $Ni(dmg)_3^{4-}$ ion in the solution, as evidenced by the precipitation of a major part of the Ni^{2+} ions as $Ni(dmgH)_2$. Complexes **1** and **2** are sparingly soluble in water with decomposition (precipitation of insoluble red solid, $Ni(dmgH)_2$) but reasonably soluble in organic solvents such as acetone, alcohols, and acetonitrile.

The nickel *vic*-dioximes, e.g. $Ni(dmgH)_2$, have appreciable IR absorptions in the region of 2300 cm^{-1} due to the OH stretching vibrations of the hydrogen-bonded OHO groups.[29] These absorptions are missing in the spectra of the trinuclear complexes, indicating that the enolic hydrogen atoms are lost on chelation. The ν(CN) vibration is assigned to the medium intense band at 1590 cm^{-1} for **1** and 1595 cm^{-1} for **2**. The ν(CN) vibration is situated at a significantly higher frequency than that for the corresponding $Ni(dmgH)_2$, where the vibration is found at 1560 cm^{-1}. This is in accord with the concept that on trinuclear complex formation the positively charged LFe^{3+} unit stabilizes the negative charge on oxygen of the oximate function[19a] and thus increases the double-bond character of the CN bond, which is expressed as a rise in the frequency. The band of medium strength at 1184 cm^{-1} is assignable to the NO stretching vibration. $Ni(dmgH)_2$ exhibits two bands of medium intensity at 1235 and 1100 cm^{-1} which have been assigned to NO stretches.[29] The second NO infrared absorption could not be observed in the perchlorate salt, **1**, because of the superposition of the strong band originating from the perchlorate anion. However, for the hexafluorophosphate salt,

Table III. Selected Bond Lengths (Å) and Angles (deg) for $[L_2Fe_2(dmg)_3Ni](PF_6)_2 \cdot 0.5CH_3OH$ with their Esd's in Parentheses

Fe(1)–Ni(1)–Fe(1a)	179.4 (2)		
Fe(1)···Fe(1a)	6.982 (2)	Fe(1)···Ni(1)	3.491 (3)
Fe(1)–O(1)	1.953 (8)	Ni(1)–Ni(1)	2.050 (17)
Fe(1)–O(2)	1.950 (12)	Ni(1)–N(2)	2.023 (17)
Fe(1)–O(3)	1.927 (12)	Ni(1)–N(3)	2.033 (17)
Fe(1)–N(4)	2.231 (16)	O(1)–N(1)	1.380 (19)
Fe(1)–N(5)	2.261 (12)	O(2)–N(2)	1.371 (20)
Fe(1)–N(6)	2.232 (17)	O(3)–N(3)	1.389 (20)
O(1)–Fe(1)–O(3)	97.0 (4)	O(1)–Fe(1)–N(4)	90.4 (4)
O(1)–Fe(1)–O(2)	98.4 (4)	O(1)–Fe(1)–N(5)	167.5 (6)
O(2)–Fe(1)–O(3)	98.5 (5)	O(1)–Fe(1)–N(6)	92.8 (4)
O(2)–Fe(1)–N(4)	89.9 (5)	O(2)–Fe(1)–N(5)	88.3 (5)
O(2)–Fe(1)–N(6)	165.1 (5)	O(3)–Fe(1)–N(4)	167.9 (5)
O(3)–Fe(1)–N(5)	92.4 (5)	O(3)–Fe(1)–N(6)	89.9 (6)
N(4)–Fe(1)–N(5)	79.0 (5)	N(4)–Fe(1)–N(6)	80.1 (6)
N(5)–Fe(1)–N(6)	79.0 (5)		
N(1)–Ni(1)–N(2)	90.8 (5)	N(1)–Ni(1)–N(3)	87.7 (5)
N(1)–Ni(1)–N(1a)	150.7 (5)	N(1)–Ni(1)–N(2a)	112.6 (5)
N(1)–Ni(1)–N(3a)	75.5 (5)	N(2)–Ni(1)–N(3)	89.7 (5)
N(2)–Ni(1)–N(2a)	76.4 (5)	N(2)–Ni(1)–N(3a)	155.2 (5)
N(3)–Ni(1)–N(3a)	109.9 (5)		

(23) SHELXTL-PLUS program package 3 by G. M. Sheldrick, Universität Göttingen, 1988. Computations were carried out on a Microvax II computer.

(24) *International Tables for X-ray Crystallography*; Kynoch: Birmingham, England, 1974; Vol. 4.

(25) The pale yellow solution affords the binuclear iron(II) complex $[L_2Fe^{II}_2(\mu\text{-}OH)(\mu\text{-}CH_3COO)_2]ClO_4 \cdot H_2O$, a model compound for the oxygen-transfer protein deoxyhemerythrin, upon addition of $NaClO_4 \cdot H_2O$.

(26) (a) Chaudhuri, P.; Wieghardt, K.; Nuber, B.; Weiss, J. *Angew. Chem., Int. Ed. Engl.* **1985**, *24*, 778. (b) Hartmann, J. R.; Rardin, R. L.; Chaudhuri, P.; Pohl, K.; Wieghardt, K.; Nuber, B.; Weiss, J.; Papaefthymiou, G. C.; Frankel, R. B.; Lippard, S. J. *J. Am. Chem. Soc.* **1987**, *109*, 7387.

(27) Attempts to isolate the very oxygen-sensitive $Fe^{II}Ni^{II}Fe^{II}$ complex are underway.

(28) Chaudhuri, P.; Winter, M.; Wieghardt, K.; Gehring, S.; Haase, W.; Nuber, B.; Weiss, J. *Inorg. Chem.* **1988**, *27*, 1564.

(29) (a) Blinc, R.; Hadzi, D. *J. Chem. Soc. A* **1958**, 4536. (b) Burger, K.; Ruff, I.; Ruff, F. *J. Inorg. Nucl. Chem.* **1965**, *27*, 179. (c) Caton, J. E.; Banks, C. V. *Inorg. Chem.* **1967**, *6*, 1670.

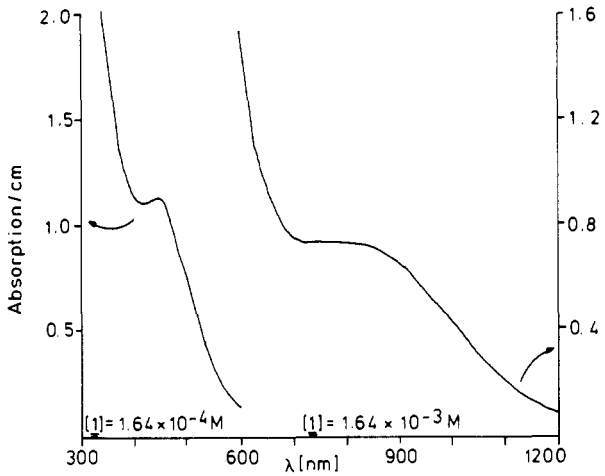

Figure 1. Electronic spectra of $[L_2Fe_2(dmg)_3Ni](ClO_4)_2$ in acetonitrile solution.

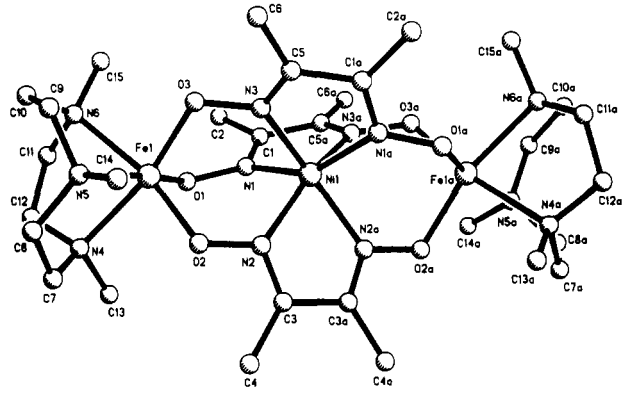

Figure 2. ORTEP drawing of the dication $[L_2Fe_2(dmg)_3Ni]^{2+}$ in **2**.

2, the second NO stretch has been identified unambiguously at 1072 cm^{-1}. The perchlorate salt shows a broad strong band at 1097 cm^{-1} (antisymmetric stretch) and a sharp band at 625 cm^{-1} (antisymmetric bend), indicative of uncoordinated perchlorate anions. Complex **2** shows a strong sharp band at 843 cm^{-1} due to the hexafluorophosphate anions.

The optical spectrum of complex **1** in acetonitrile has been measured in the 300–1200-nm wavelength range (Figure 1). Two maxima are found at 444 nm ($\epsilon \approx 6902$ M^{-1} cm^{-1}) and ≈850 nm ($\epsilon \approx 448$ M^{-1} cm^{-1}). Metal to ligand charge-transfer (MLCT) absorptions can occur in complexes where unsaturated ligands like dimethylglyoxime, which contain empty antibonding π orbitals, are bonded to oxidizable metals. On the basis of the high extinction coefficient and the relative sharpness, the peak at 444 nm is ascribed to a charge-transfer transition. The broad band at ≈850 nm is thought to be due to ligand field (d–d) transitions occurring at the central Ni(II) center. The extinction coefficient of this band is large in comparison to those for the octahedral Ni(II) complexes, probably because of the intensity gain through exchange coupling[30] and of the strong trigonal distortion[31] of the Ni(II) geometry, resulting in a lowering of symmetry from O_h to D_3. The energy of this transition is essentially insensitive to different solvents, viz. methanol, acetone, acetonitrile, and dimethyl sulfoxide, lending further support to the d–d nature of this broad band at ≈850 nm.

Description of the Structure of 2. The molecular geometry and the atom-labeling scheme of the cation are shown in Figure 2. The structure of the complex molecule consists of a discrete dicationic trinuclear centrosymmetric unit having a crystallographic 2-fold symmetry, two noncoordinatively bound hexafluorophosphate anions, and half of a methanol molecule. The

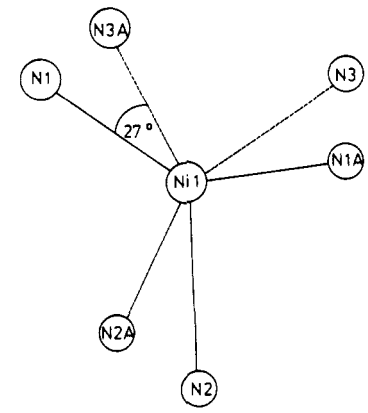

Figure 3. Triangular distortion of the NiN_6 chromophore.

X-ray structure confirms that a linear trinuclear complex (Fe(1)–Ni(1)–Fe(1a) = 179.4 (2)°) has indeed been formed in such a way that a trioctahedral geometry containing a nickel(II) and two irons(III) as central atoms is present in the lattice. The central tris(dimethylglyoximato)nickelate(II) ion, $Ni(dmg)_3^{4-}$, bridges the two terminal iron(III) centers through the deprotonated oxime oxygens. The iron coordination geometry is distorted octahedral with three nitrogen atoms from the facially coordinated tridentate amine and three oxygen atoms from three bridging oximate groups. The central nickel ion is coordinated to six imine nitrogens, and the coordination geometry is strongly trigonally distorted. Selected bond distances and angles are listed in Table III. An intramolecular Fe···Fe separation of 6.982 (2) Å has been found. The nearest *inter*molecular Fe···Fe separation is 7.37 Å. The nearest-neighbor Fe···Ni distance within the trinuclear cation is 3.491 (3) Å. The Fe–O (average 1.943 (11) Å) and Fe–N (average 2.241 (15) Å) bond lengths are very similar to those of the analogous complex[32] $[L_2Fe_2(dmg)_3Cu]^{2+}$ but are larger than those found in similar complexes with the FeN_3O_3 core, e.g. $[L_2Fe_2(\mu\text{-}CrO_4)_3]$.[28] The largest deviation from idealized 90° interbond angles is 11°, which occurs within the five-membered N–Fe–N chelate rings, the N–Fe–N angles ranging between 79.0 (5) and 80.1 (6)°, whereas the O–Fe–O angles fall between 97.0 (4) and 98.5 (5)°. The bond lengths are consistent with a d^5 high-spin electron configuration of the Fe(III) centers. The terminal Fe(1) is displaced by 0.176 (2) Å from the mean basal plane comprising N(4)N(6)O(2)O(3) atoms toward the apical nitrogen atom N(5) of the macrocyclic amine.

The mean Ni(1)–N(oxime) bond lengths (2.035 (17) Å) are larger than those found in $Ni(dmgH)_2$, 1.850 (15) Å,[33] in accordance with the greater steric requirements in the central $Ni(dmg)_3$ unit. It has been pointed out earlier[34] that the length of the Ni–N(oxime) bond is considerably dependent on whether or not the oxime proton is preserved on coordination. In the present compound, **2**, in which the oxime protons are displaced by Fe(III) centers, the Ni–N(oxime) bond distances are similar to those in comparable compounds containing undissociated oximes.[34] The central NiN_6 core is strongly trigonally distorted. The deviation from octahedral symmetry has been evaluated from the trigonal twist angle (60° for an octahedron and 0° for a trigonal-prismatic arrangement). As shown in Figure 3 the six nitrogen atoms are arranged around the Ni(II) center with a twist angle of 27° between the two triangular faces comprising N(1)N(2)N(3) and N(1a)N(2a)N(3a) atoms, respectively. In other words, the coordination polyhedron around Ni(II) is 33° away from octahedral symmetry. The Ni(II) ion lies strictly on the

(30) McCarthy, P. J.; Güdel, H. U. *Coord. Chem. Rev.* **1988**, *88*, 69.
(31) Lever, A. B. P. *Inorganic Electronic Spectroscopy*; Elsevier: Amsterdam, 1984.
(32) Chaudhuri, P.; Winter, M.; Fleischhauer, P.; Haase, W.; Flörke, U.; Haupt, H.-J. *J. Chem. Soc., Chem. Commun.* **1990**, 1728.
(33) (a) Godycki, L. E.; Rundle, R. E. *Acta Crystallogr.* **1953**, *6*, 487. (b) Williams, D. E.; Wohlauer, G.; Rundle, R. E. *J. Am. Chem. Soc.* **1959**, *81*, 755.
(34) Saarinen, H.; Korvenranta, J.; Näsäkkälä, E. *Acta Chem. Scand.* **1980**, *A34*, 443 and references therein.
(35) König, E.; König, G. In *Landolt-Börnstein*; Hellwege, K.-H., Hellwege, A. M., Springer-Verlag: Eds.; Berlin, 1981; Vol. 11.

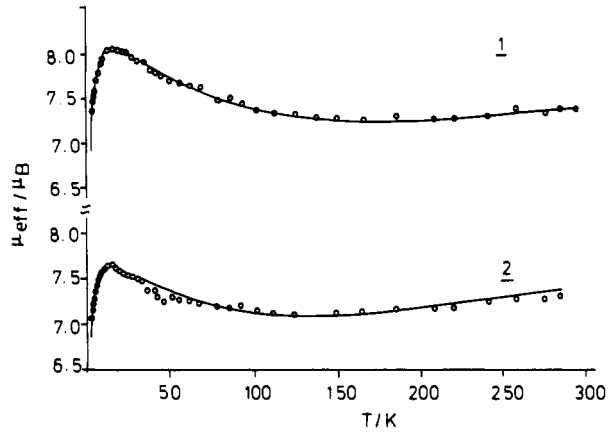

Figure 4. Plots of μ_{eff} vs T for solid **1** and **2**. The solid lines represent the best least-squares fits of the experimental data to the theoretical equation.

mean plane containing the N(2), N(3), N(2a), and N(3a) atoms. The dihedral angle between the plane N(4)N(6)O(3)O(2) containing the Fe(III) ion and the plane N(2)N(3)N(3a)N(2a) containing the Ni(II) ion is 69.3°.

The C—N (average 1.472 (20) Å) and C—C (average 1.480 (25) Å) bond lengths between the methylene groups of the macrocyclic amine L are unremarkable. The N—O (average 1.380(20) Å) and C=N (average 1.285(18) Å) bond lengths and the C–N–O bond angle (average 115.5 (11)°) of the bridging dimethylglyoximate ligands are found to be very similar to those of $Ni(dmgH)_2$ and other comparable structures.

Magnetic Susceptibility Studies. Magnetic susceptibility data for polycrystalline samples of **1** and **2** were collected in the temperature range 4.2–284.5 K, and the data are displayed in Figure 4 as μ_{eff} vs temperature. At 284.5 K the μ_{eff} values are 7.41 μ_B for the perchlorate salt, **1**, and 7.39 μ_B for the hexafluorophosphate salt, **2**. These values are much lower than the value μ_{eff} = 8.83 μ_B expected for two spins $^5/_2$ and one spin 1 with average g = 2.0. On lowering of the temperature, μ_{eff} decreases monotonically, approaching a broad minimum around 160 K, and increases upon further cooling. The plots exhibit the expected minimum.[46] The temperature behavior of the magnetic susceptibility of [Fe^{III}-$Ni^{II}Fe^{III}$], **1** and **2**, clearly indicates that the S = 1 of nickel(II) is antiferromagnetically coupled to the terminal $S = {}^5/_2$ of the iron(III) ions. μ_{eff} reaches a maximum with a value of 8.07 μ_B ($\chi_M T$ = 8.14 cm^3 mol^{-1} K) for **1** and 7.87 μ_B ($\chi_M T$ = 7.74 cm^3 mol^{-1} K) for **2** at 15.8 K. These maximum μ_{eff} values are not very close to the value of μ_{eff} = 8.93 μ_B for S = 4, which is expected as the ground state for an antiferromagnetically coupled Fe^{III}-$Ni^{II}Fe^{III}$ complex. Below 15.8 K, there is a decrease in μ_{eff}, which reaches a value of 7.37 μ_B for **1** and 7.07 μ_B for **2** at 4.1 K. Thus the magnetic behavior of **1** and **2** below 15 K can be attributed to the splitting in zero field of the ground state.

The susceptibility of [$Fe^{III}Ni^{II}Fe^{III}$][47] was calculated using the standard formula for χ_M for three linearly coupled spins with J_{12} = J_{23} = J and J_{13}, which results from the spin Hamiltonian

$$\hat{H} = -2J(\hat{S}_1\cdot\hat{S}_2 + \hat{S}_2\cdot\hat{S}_3) - 2J_{13}(\hat{S}_1\cdot\hat{S}_3)$$

for an isotropic magnetic exchange with $S_1 = S_3 = {}^5/_2$ and S_2 = 1. In this notation, J represents the exchange interaction between adjacent iron and nickel ions and J_{13} describes the interaction between the terminal iron nuclei within the trinuclear complex, shown pictorially as follows:

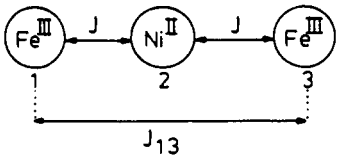

To fit the low-temperature (T < 15 K) data, it was necessary to consider a constant Θ. The expression used is

$$\chi_{calcd}^{FeNiFe} = \frac{C}{T-\Theta} f(J,J_{13},T)$$

where $C = Ng^2\mu_B^2/k$ and $f(J,J_{13},T)$ is derived from the theoretical equation. The theoretical values of χ result from the Kambe vector-coupling scheme combined with the van Vleck susceptibility equation. The experimental values of χ have been fitted to this equation by treating J, J_{13}, and the Weiss constant Θ as adjustable parameters. The Zeeman interaction of the high-spin ferric ion in a $^6A_1$ ground state with practically no contribution from orbital angular momentum is isotropic; the observed g_{Fe} values[35] are very close to the free-electron spin value of 2.0. Hence we have fixed molecular g to 2.0. Moreover, local g_{Fe} dominates over local g_{Ni} in the molecular **g** tensor expression (vide infra). The agreement between the calculated and observed magnetic susceptibilities is good, and the best fits are shown as solids lines in Figure 4. The best fit parameters are J_{Fe-Ni} = −32 (2) cm^{-1}, J_{Fe-Fe} = −5 (1) cm^{-1}, and Θ = −2.0 (1) K for **1** and J_{Fe-Ni} = −29 (2) cm^{-1}, J_{Fe-Fe} = −5 (1) cm^{-1}, and Θ = −2.1 (1) K for **2**. The deviations shown in parentheses are derived from three independent measurements.

By use of the vector-coupling models,[36,37] the **g** tensor associated with different states can be related to local spins, g_{Fe} and g_{Ni}, and is given as follows for an S = 4 ground multiplet:

$$g_{4,5} = {}^6/_5 g_{Fe} - {}^1/_5 g_{Ni}$$

The coefficients $^6/_5$ and $^{-1}/_5$ show that local g_{Fe} dominates over g_{Ni} in determining the g values of the trinuclear complex Fe^{III}-$Ni^{II}Fe^{III}$, thus lending support for fixing g = 2.0 in the fitting procedure.

Now, we would like to compare our data with the only other structurally characterized heterobimetallic $Fe^{III}Ni^{II}$ complex.[38] The J value of −12 cm^{-1} has been reported for this bimetallic complex. The evaluated coupling constants $|J|$ for **1** and **2** are larger than the $|J|$ value reported[38] for the $Fe^{III}Ni^{II}$ complex, although the Fe···Ni separation is shorter (3.38 Å) in the binuclear complex than that in our $Fe^{III}Ni^{II}Fe^{III}$ complex, **2** (3.49 Å). On the other hand, the $|J|$ values for **1** and **2** are smaller than that found for the isostructural $Fe^{III}Cu^{II}Fe^{III}$ complex (J_{Fe-Cu} = −42 cm^{-1}).[32] The increase in $|J|$ values on replacing Ni(II) by Cu(II) in an isostructural heterobimetallic series has also been observed earlier by us[39] and others.[40,41] The decrease of the exchange interactions $|J_{Fe-Cu}| > |J_{Fe-Ni}|$ is justified both by intrinsic differences between the metal ions and by the fact that the exchange-coupling constant can be expressed[42] as

$$J \propto \frac{1}{n}\sum_r J_{x^2-y^2,r}$$

where n is the number of magnetic orbitals, r, on M, if the only efficient pathway involves the $x^2 - y^2$ orbitals.

The fact that the susceptibility data for **1** and **2** cannot be well-fitted with a single coupling constant and the similarity of the obtained J_{Fe-Fe} values to those previously reported[32] for isostructural $Fe^{III}Zn^{II}Fe^{III}$ and $Fe^{III}Fe^{II}_{ls}Fe^{III}$ complexes suggest that indeed there are two different coupling constants; J_{Fe-Fe} is operative between two terminal iron centers separated by as large as 6.98 Å, which is definitely not the limit for the intramolecular magnetic interaction.[43]

A spin ladder, without the effect of J_{13} on the energy-splitting pattern, appropriate for **1** is shown in Figure 5. In Figure 5 we have also indicated the relations between molecular $\mathbf{g}_{s,s'}$ tensors

(36) Bencini, A.; Gatteschi, D. *Electron Paramagnetic Resonance of Exchange Coupled Systems*; Springer-Verlag: Berlin, 1990.
(37) Scaringe, R. P.; Hodgson, D. J.; Hatfield, W. E. *Mol. Phys.* **1978**, *35*, 701.
(38) Holman, T. R.; Juarez-Garcia, C.; Hendrich, M. P.; Que, L., Jr.; Münck, E. *J. Am. Chem. Soc.* **1990**, *112*, 7611.
(39) Chaudhuri, P.; Winter, M.; Küppers, H.-J.; Wieghardt, K.; Nuber, B.; Weiss, J. *Inorg. Chem.* **1987**, *26*, 3302.
(40) Bencini, A.; Benelli, C.; Gatteschi, D.; Zanchini, C.; Fabretti, A. C.; Franchini, G. C. *Inorg. Chim. Acta* **1984**, *86*, 169.
(41) Journaux, Y.; Slelten, J.; Kahn, O. *Inorg. Chem.* **1986**, *25*, 439.
(42) Girerd, J. J.; Charlot, M. F.; Kahn, O. *Mol. Phys.* **1977**, *34*, 1063.
(43) Chaudhuri, P.; Oder, K.; Wieghardt, K.; Gehring, S.; Haase, W.; Nuber, B.; Weiss, J. *J. Am. Chem. Soc.* **1988**, *110*, 3657.

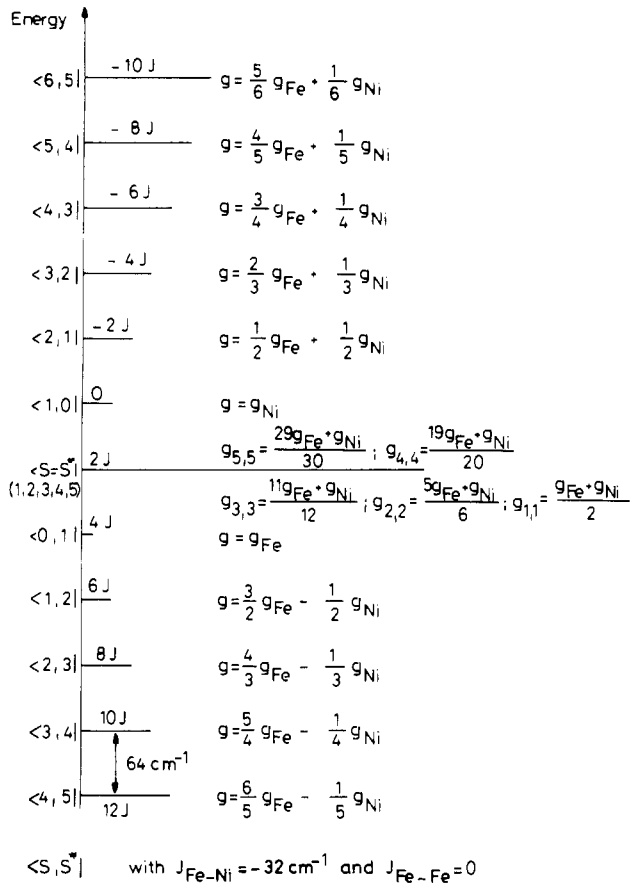

Figure 5. Spin ladder appropriate for $[L_2Fe_2(dmg)_3Ni](ClO_4)_2$. The degeneracies of the levels are expressed by the lengths of the corresponding lines. For each level the relation between molecular g_{S,S^*} and local g_{Fe} and g_{Ni} has been included.

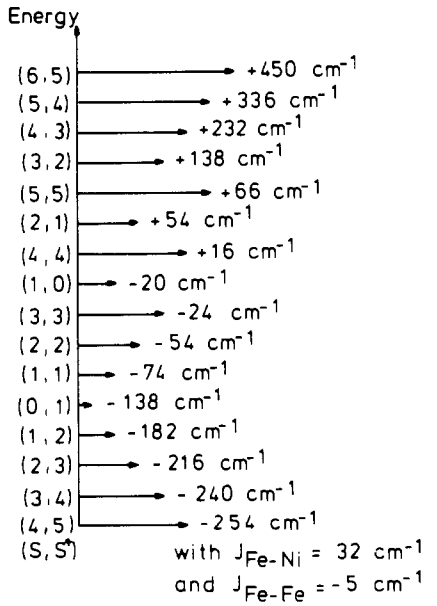

Figure 6. Effects of J_{Fe-Fe} on the energy-splitting pattern (not to scale) of Figure 5.

and local g_{Fe} and g_{Ni} values. S^* is defined by the relation $S^* = S_{Fe} + S_{Fe}$, and $S = S^* + S_{Ni}$ is the total molecular spin. The most pronounced effect of J_{13} is to lift the degeneracy of the central levels with $S = S^*$, which has also been reported earlier.[44] As is evident from Figure 6, the effect of an antiferromagnetic J_{13} on the splitting pattern is to raise the ground-state levels with high

(44) Herren, M.; Jacobsen, S. M.; Güdel, H. U. *Inorg. Chem.* **1989**, *28*, 504.

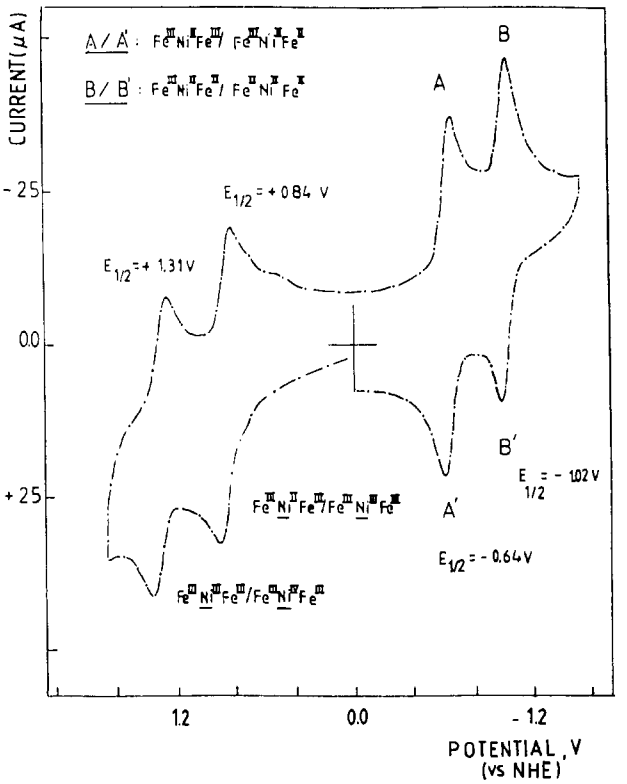

Figure 7. Cyclic voltammogram of **1** in CH_3CN at a scan rate of 0.2 V s^{-1}.

S in energy and to lower the energy of the levels with low-S quantum numbers. Thus the energy difference between the ground state $|S^* = 5, S = 4\rangle$ and the next upper-lying level $|S^* = 4, S = 3\rangle$ of 64 cm^{-1} becomes reduced to 14 cm^{-1} in **1** by the effect of J_{Fe-Fe} on the energy splittings (Figures 5 and 6).

The Fe···Ni separation of 3.49 Å in **2** is so large that the exchange integral cannot originate from direct Fe–Ni interaction. Thus, the observed spin coupling is likely to arise through a superexchange mechanism operating via the Fe^{III}–O–N–Ni^{II}–N–O–Fe^{III} linkages. The antiferromagnetic interactions in **1** and **2** can be interpreted by considering that the e_g orbitals of the Fe(III) ions point from the metal toward the six donor atoms (N_3O_3) and overlap on either side of the three bridging glyoximato ligands, which favor an antiferromagnetic interaction. Weaker interactions in **1** and **2** in comparison to that in the similar $Fe^{III}Cu^{II}Fe^{III}$ complex[32] can be rationalized by envisaging that the d_{z^2} orbital of the central Ni(II) ion in $Fe^{III}Ni^{II}Fe^{III}$ provides a ferromagnetic contribution to the overall exchange interaction, hence causing a reduction in the overall antiferromagnetic interaction in **1** and **2**, whereas the d_{z^2} orbital of the Cu(II) ion in $Fe^{III}Cu^{II}Fe^{III}$ is fully occupied by a pair of electrons. In other words, the overlap between the magnetic orbital on Fe(III) and that on Ni(II), in $Ni(dmg)_3^{4-}$, is essentially σ in nature, and hence the extent of the coupling should be independent of the dihedral angle between the two equatorial planes containing Fe(III) and Ni(II), respectively, as is evident from the solid-state structures of the binuclear $Fe^{III}Ni^{II}$ and the trinuclear $Fe^{III}Ni^{II}Fe^{III}$ complex.

Electrochemistry. The cyclic voltammogram of $Fe^{III}Ni^{II}Fe^{III}$ at ambient temperature in CH_3CN containing 0.1 M tetra-*n*-butylammonium hexafluorophosphate as supporting electrolyte at a glassy carbon working electrode at a scan rate $v = 0.2$ V s^{-1} is shown in Figure 7. Two consecutive reversible steps of reduction in the potential range 0.0 to −1.6 V at $E_{1/2}^{red1} = -0.64$ V and $E_{1/2}^{red2} = -1.02$ V vs NHE are detected. That two reversible transfers of one electron per center occurs is evident from the adherence to the following criteria:[45] (i) the $E_{1/2}$ values are

(45) (a) Nicholson, R. S.; Shain, I. *Anal. Chem.* **1964**, *36*, 706. (b) Bard, A. J.; Faulkner, L. R. *Electrochemical Methods: Fundamentals and Applications*; Wiley: New York, 1980.

independent of scan rates between 20 mV s^{-1} and 1 V s^{-1}, −0.50 and −0.885 V vs Ag/AgCl; (ii) the difference in peak potential values ΔE_p ($=E_{pa} - E_{pc}$) is constant and equal to 65 mV; (iii) the ratio of the peak currents due to cathodic (i_{pc}) and anodic (i_{pa}) sweeps is close to unity (1.00 ± 0.02) at different scan rates; (iv) the current function $i_p v^{-1/2}$ is substantially constant. The formal redox potentials thus obtained can be regarded as thermodynamic values. Thus the following redox scheme, containing the reversible formation of a mixed-valent $Fe^{III}Ni^{II}Fe^{II}$ species, can be ascribed to the electrochemcial reduction processes of the complex $Fe^{III}Ni^{II}Fe^{III}$:

$$Fe^{III}Ni^{II}Fe^{III} \overset{E_{1/2}^{red1}}{\rightleftharpoons} Fe^{III}Ni^{II}Fe^{II} \overset{E_{1/2}^{red2}}{\rightleftharpoons} Fe^{II}Ni^{II}Fe^{II}$$

Electrochemically reversible one-electron-transfer steps ($\Delta E_p \approx$ 65 mV) preclude any significant structural rearrangement during the redox processes; i.e., all three species have the same structures in solution and apparently can be described by the solid-state structure of the $Fe^{III}Ni^{II}Fe^{III}$ complex as determined by X-ray diffraction. No reduction current from Ni(II) to Ni(I) is observed in the potential range 0.0 to −2.0 V vs NHE.

Analyses of the cyclic voltammograms in the positive potential range (0.0 to +1.5 V) with scan rates varying from 0.02 to 1 V s^{-1} reveal that (i) the peak current ratio i_{pa}/i_{pc} is constant (1.00 ± 0.04), (ii) the current function $i_p v^{-1/2}$ is virtually constant and independent of scan rates, and (iii) the peak potential difference, ΔE_p, increases progressively from 60 to 115 mV with scan rates 0.02 to 1 V s^{-1}, respectively. These findings clearly indicate a simple one-electron mechanism for the oxidation processes, quasi-reversible in character. Thus two quasi-reversible oxidation processes at $E_{1/2}^{ox1}$ = +0.84 V and $E_{1/2}^{ox2}$ = +1.31 V vs NHE, which can be assigned to the equilibria

$$Fe^{III}Ni^{II}Fe^{III} \overset{E_{1/2}^{ox1}}{\rightleftharpoons} Fe^{III}Ni^{III}Fe^{III} \overset{E_{1/2}^{ox2}}{\rightleftharpoons} Fe^{III}Ni^{IV}Fe^{III}$$

are observed. The quasi-reversible character of these redox reactions indicates that some geometrical changes are taking place without changing the actual framework of the structure. On the contrary, for $Ni(dmgH)_2$ two processes, both with $E_{qr}Ci$, are observed. The couple localized at −1.44 V corresponds to the reduction of Ni(II) to Ni(I) and the couple at +1.14 V corresponds to the oxidation from Ni(II) to Ni(III). The shift of 300 mV to more negative potential for the couple Ni(II)/Ni(III) in the $Fe^{III}Ni^{II}Fe^{III}$ complex in comparison to $Ni(dmgH)_2$ probably causes the stabilization of the $Fe^{III}Ni^{IV}Fe^{III}$ species.

Concluding Remarks

In this paper a unique linear trinuclear $Fe^{III}Ni^{II}Fe^{III}$ compound is described that can provide a suitable basis for further research, especially on the electronic properties of such a trinuclear system. That it is possible to stabilize tris(dimethylglyoximato)nickelate(4−) anion by complexing with the LFe^{3+} unit has been demonstrated. Recently, another series of glyoximato-bridged[20] trinuclear complexes of general formula $[L_2Cu_2(dmg)_2M^{II}]^{2+}$ (M = Cu, Ni, Pd) has been described. (Glyoximato)metalate(II) anions are capable of functioning as bridging ligands to give rise to various kinds of trinuclear complexes and can mediate a varying range of exchange, from very weak to very strong antiferromagnetic interactions. Our study on the low-lying electronic states of $[L_2Fe^{III}_2(dmg)_3Ni^{II}]X_2$ (X = ClO_4, PF_6) by magnetic susceptibility shows that the complex contains two high-spin ferric sites which are antiferromagnetically coupled to a high-spin Ni(II), yielding a coupling constant $J \approx -30$ cm^{-1}. This study also suggests that there are indeed two different coupling constants $J_{12} = J_{23} = J$ and J_{13} operative in the $Fe^{III}Ni^{II}Fe^{III}$ complex; J_{13} is operative between two terminal iron centers separated by as large as 6.98 Å. This paper confirms the essentially σ nature of the Fe(III)–Ni(dmg) interaction. The spin-level structure of the compound is characterized by the ferromagnetic-like polarization of high local spins.[46] In fact, there are no truly ferromagnetic interactions in the trinuclear complex. Both J_{Fe-Ni} and J_{Fe-Fe} are antiferromagnetic. The ordering of energy levels follows from the fact that the Fe(III) ($S_{Fe} = {}^5/_2$) magnetic moments are larger than those of Ni(II) ($S_{Ni} = 1$). The level ordering is a result of the mutual influence of the Fe^{III}–Ni^{II} interactions, J_{Fe-Ni}, and the Fe^{III}–Fe^{III} interactions, J_{Fe-Fe}. The oxidized species $Fe^{III}Ni^{III}Fe^{III}$ and $Fe^{III}Ni^{IV}Fe^{III}$ and the reduced species $Fe^{II}Ni^{II}Fe^{III}$ and $Fe^{II}Ni^{II}Fe^{II}$ have been observed in cyclic voltammetric experiments. The chemical preparations and isolation of the $Fe^{III}Ni^{III}Fe^{III}$ and $Fe^{II}Ni^{II}Fe^{II}$ species seem possible. These investigations are in progress.

Acknowledgment. P.C. is thankful to Prof. K. Wieghardt for his help and interest. Financial support from the DFG (Grant Ch 111/1-1) is gratefully acknowledged.

Registry No. **1**, 131997-03-0; **2**, 136762-69-1; $LFeCl_3$, 110827-37-7; $Ni(dmgH)_2$, 13478-93-8; $[L_2FeNi(dmg)_3]^+$, 136762-66-8; $L_2FeNi(dmg)_3$, 136762-70-4.

Supplementary Material Available: Summary of crystal data and intensity measurements (Table SI) and listings of intraligand bond distances and angles (Tables SII and SIII), anisotropic thermal parameters (Table SIV), and hydrogen atom coordinates (Table SV) (8 pages); a listing of observed and calculated structure factors (15 pages). Ordering information is given on any current masthead page.

(46) Pei, Y.; Journaux, Y.; Kahn, O. *Inorg. Chem.* **1988**, *27*, 399.

(47) The model adopted for the analysis of the magnetic susceptibility data has some limitations, e.g. the neglect of zero-field splitting. But the zero-field splitting of the ground state is not appreciable, as is indicated by observation of the X-band EPR spectra, which together with $[Fe^{III}Mn^{II}Fe^{III}]$, $[Fe^{III}Fe^{II}_{ls}Fe^{III}]$, and $[Fe^{III}Zn^{II}Fe^{III}]$ will be the subject of a forthcoming paper.